

STRESS DEVELOPMENTS IN LARGE TIMBER CROSS SECTIONS IN RELATION TO GEOMETRY AND ENCOUNTERED CLIMATE

Bettina Franke¹, Marcus Schiere², Steffen Franke³

ABSTRACT: Timber cross sections are found in all kinds of sizes and dimensions and are subjected to a wide range of ambient climate conditions. This leads to questions regarding safety of timber structures in all the different applications, either in heated or sheltered climate. Studies have been performed on response of glued laminated timber cross sections to changes in these climates, causing swelling and shrinkage and corresponding stresses perpendicular to the grain. The allowable tensile stress limits in this material direction are low. Along with the experiments performed in laboratories, simulations in finite element methods were performed to investigate the effect of the different climates on large cross sections. It was found that tensile stresses perpendicular to the grain easily develop in the outer cross sections of beams with any type of geometry in drying conditions. In the inner part of cross sections, the magnitude of stresses perpendicular to the grain depends much on the geometry.

KEYWORDS: Local climate, building standards, moisture content, moisture induced stresses, cross section geometry

1 INTRODUCTION

Wood is a construction material used in the past, present and future. Knowledge and experience on design and planning accounting for constant and variable structural loads has been built up in the past. However, knowledge on the hygroscopic behaviour of wood in the field of construction and quality assurance needs to be increased. Wood shrinks or swells due to variations in surrounding humidity.

Wood is also a hygroscopic material that will adsorb and desorb moisture as surrounding relative humidity changes. Moisture content (MC) affects material strength, stiffness, and long-term structural deformation to which measures must be taken according to EN 1995 (Eurocode 5) [1] or SIA 265 [2] through Service Classes: Service Class 1 for average moisture content under 12 M%, Service class 2 for moisture contents between 12 M% and 20 M%, and Service Class 3 for moisture contents above 20 M%. The importance of the relation between MC and structural damage is shown through an assessment of many buildings where MC changes, high MC, or low MC could implicitly be related to almost half of the evaluated cases of structural damage or failure [3]. A similar study showed that MC changes accounted for about one third of the previously mentioned

50% [4]. Apart from moisture content variations during regular operation of the structure, special events such as erection time and possible maintenance have to be considered.

As the distribution of the MC across the member is often non-uniform, so is the anisotropic hygro-expansion and stiffness, internal stresses perpendicular to the grain are generated known as moisture induced stresses (MIS), see Figure 1. The figure illustrates a wetting process and the generation of compression stresses at the surface followed by the tension stresses in the midplane of the glued laminated cross sections.

These stresses can exceed the characteristic tensile strength of 0.4 N/mm^2 of timber perpendicular to the grain [2] as shown experimentally and initiate cracks perpendicular to the grain [5][6]. Small changes of moisture content can already lead to stresses exceeding the tension strength of timber perpendicular to the grain [7]. In many cases the dimensions of a beam loaded in bending will be dominated by the bending stresses and to a

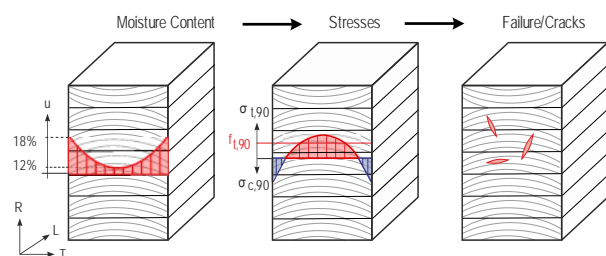


Figure 1: Illustration moisture content distribution during a wetting processes (left), the development of compression stresses on the surface and the tension stresses in the midplane (middle), and the initiation of cracks perpendicular to grain (right).

¹ Bettina Franke, Institute for Architecture, Timber construction and Structures, Bern University of Applied Sciences, bettina.franke@bfh.ch

² Marcus Schiere, Institute for Architecture, Timber construction and Structures, Bern University of Applied Sciences, marcusjacob.schiere@bfh.ch

³ Steffen Franke, Professor for timber structures, Institute for Architecture, Timber construction and Structures, Bern University of Applied Sciences, steffen.franke@bfh.ch

lesser degree by the shear stresses. However, in cases where loads are suspended from such a member and cause tensile stresses, or tensile stresses are caused by the beam being curved or tapered, these must be handled carefully. In curved and notched beams, laboratory tests have shown that these stresses can directly lead to total failure [8][9]. Repairs or reinforcements can be made if damage is detected in time [10].

The study starts with a discussion of climates and geometries found in practice. This is accompanied with experimental results to explain the moisture content developments in large glued laminated cross sections. Numerical simulations are performed to understand relations between geometry and magnitude of the MIS caused by the swelling and shrinkage. These are more difficult and time consuming to measure. Experimental results for smaller glulam cross sections are however available. For now, the text will focus on the magnitude of the stresses in different geometries and different ambient climate conditions. Maximum allowable stress limits are not given. The simulations are performed using Finite Element Methods.

2 STATE OF THE ART

2.1 MONITORED STRUCTURES

The subdivision of material properties into service classes was explained in the introduction. Roughly, Service Class 1 is appropriate for structures that are heated in winter. Service Class 2 structures are ventilated throughout the year and not heated during winter. Monitoring campaigns in which temperature and relative humidity have been measured along with the moisture contents in large heated and unheated structures, bridges too [11][12], see Figure 2. The figure shows an overview of representative mean annual moisture contents measured in different large span timber structures. The maxima and minima are also shown, along with the limits of the moisture contents suggested by the Service Classes [1].

On top of this, new unheated structures were recently instrumented (1) structures located in climates where relative humidities were over 90 %RH for large parts of

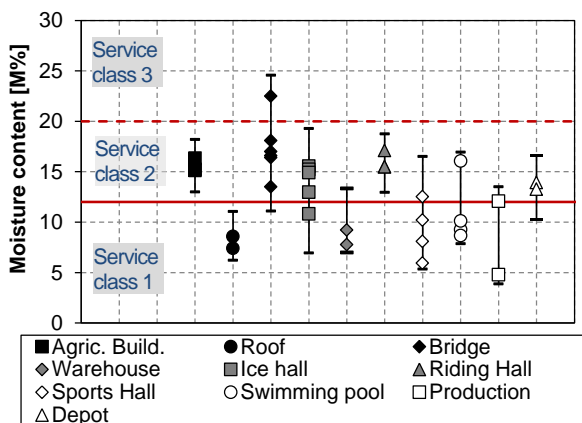


Figure 2: Measured average moisture contents in load bearing elements in different applications. Minima and maximum annual values are shown as well as limits of the different Service Classes [1][11][12].

the year, (2) structures located at high altitudes of 1500 m above sea level, and (3) bridges [13]. Data obtained from this the new monitoring campaigns does not span a long period yet, so it is not included in Figure 2.

Relative humidities in Service Class 1 structures is below 65 %RH in winter, and as relative humidity in summer is quite low when buildings are ventilated for instance, structures do not become very humid throughout the year. The ventilation in Service Class 2 structures causes relative humidities in the colder months to rise above 65 %RH set as maximum in the Service Class 1.

2.2 TIMBER CROSS SECTIONS

The load bearing timber members studied are the large timber cross sections used in large span halls and bridges, see Figure 3 and Figure 4. It is often more economic to install several large load bearing members in the structures as multiple smaller ones. This results in cross sections of 200+ mm wide and 2000 mm deep. Some are assembled into block glulam beams as well, where two beams or more beams are joined to form very wide cross sections. Figure 4 gives an idea of cross section sizes used over the last 50 years in more modern bridges. It

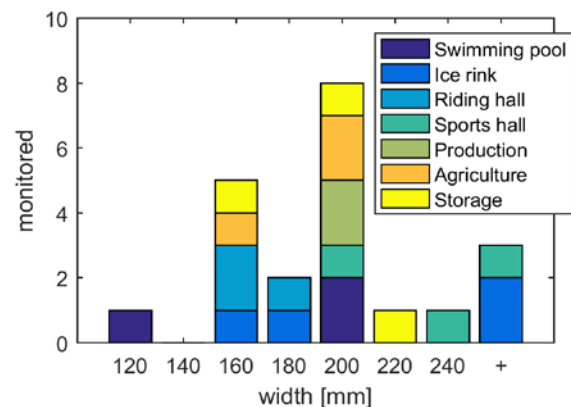


Figure 3: Distribution of monitored cross section widths in large span structures of different use [12].

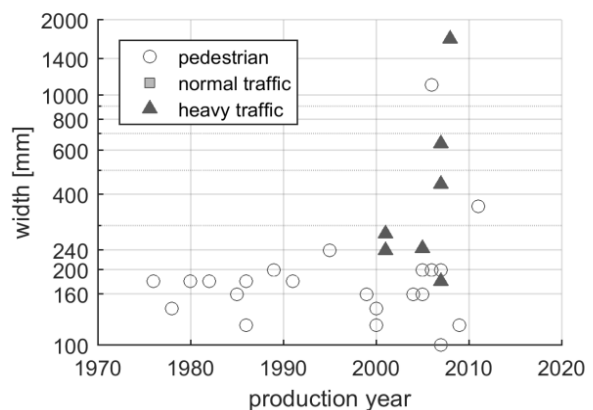


Figure 4: Illustration of increase of width of cross sections used in different types of bridges. Eventually, block glulam beams are used to transfer the high loads traffic up to 40 tons. [14]

shows that cross section widths are slowly increasing, until these are finally block glued into very large cross sections more than 1.5 m wide. These are cross sections of all types of bridges: arch bridges, truss bridges, etc. [14].

2.3 STRESS DISTRIBUTION AND DAMAGE INITIATION

Weibull weakest link stress approaches have been used in earlier studies to estimate the fracture of curved and notched beams located in varying ambient climates [8]. Weibull weakest link stress approaches have also been used in beams with internal stress distributions that are not loaded externally. It is imaginable that Weibull weakest link theory does not fully apply to these cases as the cross section is loaded both in tension and compression. The correct estimation of crack initiation can be quite complex involving factors like volume, load history and moisture content too. The latter is especially though to be a challenge as there is a negative dependency of strength of approximately 3%/M%, with a peak at 10 M% [6][15].

The Eurocode 5 defines a characteristic tensile strength perpendicular to the grain of 0.4 N/mm² for a reference volume of 1 dm³ for glued laminated timber loaded in tension. Experiments and simulations have shown that this stress levels are easily achieved [5][6]. Higher stress limits can be used, based for instance on material density [22]. Although differences between stress limits in radial and tangential direction exist, these often not distinguished [15].

3 EXPERIMENTS AND SIMULATIONS

3.1 EXPERIMENTS

To observe the development of moisture content over large cross section, a test specimen of four block glued glulam members of 200 x 800 x 600 mm³ (width x height x length) was produced. The longitudinal (*L*) side faces were sealed, so that the moisture diffusion only could take place in radial (*R*) and tangential (*T*) directions. The specimens represent a middle part of a structural member. Measurement gages to measure moisture content, temperature and strain were installed. The gages were installed at midplane from the sealed surfaces along the radial-, and tangential directions as well as diagonal in between radial and tangential, as shown in Figure 5 [7]. The directions are indicated with *R*, *T*, and *RT* letters respectively. The number behind the letter represents the depth from the surface in millimetres.

The electrical resistance method was used to determine the moisture content developments using a pair of partly insulated stainless-steel electrodes as sensor. The single glulam beams were conditioned in 20 °C and 65 % relative humidity for several weeks before being instrumented and glued together to form the lock glulam beam. Afterwards, the beam was consecutively put in three different climates: (1) adsorption process in 20 °C and 85 % relative humidity; (2) desorption process in 20 °C and 50 % relative humidity; and (3) a sheltered outside climate, starting in winter and ending in autumn, in the premises of the Bern University of Applied Sciences.

The duration of each of the three intervals was around 10 month each.

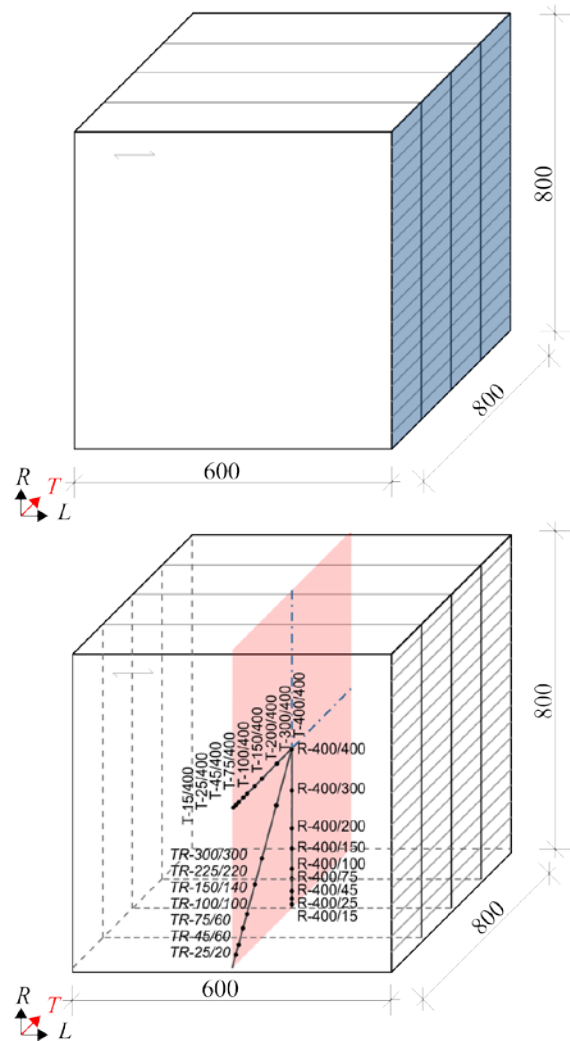


Figure 5: Principle sketch of block glued test specimen, location and orientation of measuring points and installation of measuring devices.

3.2 NUMERICAL MODEL

3.2.1 Moisture transport

Simulations were carried out to estimate the stresses and find the important factors affecting the tensile stress levels. Such a variation can include board layup, applied climate load, hygro-expansion factors, geometry, etc. These can then also be compared to experimental data [5][16]. Numerical models to calculate the moisture content distributions and corresponding moisture induced stresses are available in literature: such as a 1D model in [17], 2D-model in [16], and 3D-model in [18]. For this study, a 2D model will be used. To calculate the moisture content distribution, Fick's second law for diffusion is used.

$$\frac{\partial u}{\partial t} = D \frac{\partial^2 u}{\partial x^2} \quad (1)$$

In which u refers to MC, D to diffusion, and t and x to time and space respectively. Many parameters for factor D can be chosen [19][20], however, relatively high values will be used to accelerate stress generation and allow to focus on trends. The boundary conditions at the surface of a cross section is assumed to be equal to the theoretical equilibrium moisture content calculated from the relative humidity and temperature. This is valid for wetting in all conditions, and drying in ventilated areas where air velocity is larger than 3 m/s. No surface resistance is assumed to facilitate the analysis later on. Advanced approaches through which moisture content developments can be modeled in dynamic ambient conditions are can be found in literature though.

3.2.2 Strain and stress

The moisture induced stresses are calculated using the derivative of total strain to time, in which the total strain $\dot{\epsilon}_t$ is the sum of elastic strain $\dot{\epsilon}_E$, hygro-expansive strain $\dot{\epsilon}_u$, mechano-sorptive strain $\dot{\epsilon}_{ms}$, and creep strain $\dot{\epsilon}_\varphi$, as given in Eq. (2).

$$\begin{aligned}\dot{\epsilon}_t &= \dot{\epsilon}_E + \dot{\epsilon}_u + \dot{\epsilon}_{ms} + \dot{\epsilon}_\varphi \\ \dot{\epsilon}_t &= \frac{\dot{\sigma}}{E} + \alpha \dot{u} + m \dot{u} \sigma + 0\end{aligned}\quad (2)$$

In which E represents the anisotropic elasticity matrix, α is a vector with the hygro-expansive factors, and m is a matrix with the mechano-sorptive creep as a function of moisture transport times the stress. The creep strain in these dynamic conditions is often discarded [17].

These equations above can be implemented into a coupled thermal-structural or concentration-structural analysis in ANSYS®. The mechano-sorptive strains are added by using pre-strain algorithms [21]. Material behaviour is expected to stay elastic and material elasticity is constant throughout the range of moisture contents achieved.

3.2.3 Material parameters

A list of the material parameters is given in Table 1. The material parameters were obtained from [16][18].

Table 1: List of material parameters used in the numerical model

parameter	Value	Parameter	Value
E_r [N/mm ²]	467	D [m ² /s]	3e-10
E_t [N/mm ²]	216	m_r [mm ² /N]	0.07e-6
G_{rt} [N/mm ²]	42	m_t [mm ² /N]	0.10e-6
nu_{rt} [N/mm ²]	0.50	m_{rt} [mm ² /N]	0.40e-6
α_r [%/M%]	0.13	mu_{tr}	0.75
α_t [%/M%]	0.32	mu_{rt}	0.75

3.3 EVALUATION OF STRESS DISTRIBUTION

The obtained stress distributions in beams with high aspect ratios are normally only relevant in vertical direction, i.e. σ_y , see Figure 6. In the evaluation of the tresses

in the block glulam beams, stresses in the horizontal direction, σ_x , will also start to increase. To account for the stress developments in both beam directions in one single parameter, σ_t (subscript t for tensile), the stresses are evaluated according to the diagram shown in Figure 6. This diagram divides the stresses in vertical and horizontal direction of the beam in four different quadrants. It is noted that in the bottom left quadrant, during compression in both directions, σ_t will be 0. In the upper right quadrant, when stress in both directions is positive, the square root of the squared stresses in each direction is used. In the other two quadrants, the tensile stress of the corresponding direction will be used.

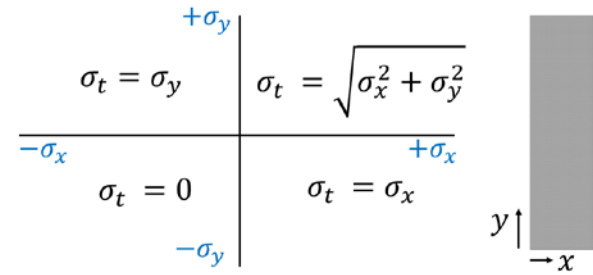


Figure 6: Illustration of how stresses are evaluated when these are expected to be large in two different directions

3.4 SIMULATED CROSS SECTIONS AND USED LOADS

A set of numerical simulations was made to investigate the dependency of dimension and layup on the development of moisture induced stresses, see also Figure 7:

- Three variation of cross section widths are made of 160 mm, 200 mm, and 240 mm using a step load of 6 M%. The layup was in ideal: all piths were in the midplane and 30 mm under the board. Aspect ratio of height over width of $\lambda = 4$.
- Three variations were made in which the annual ring angle stayed constant at the surface while cross section width was varied from 160 mm, 200 mm, and 240 mm. Piths were all in the midplane but distance from the board edge had to be increased according to the cross section. Applied moisture change was 6 M% and aspect ratio $\lambda = 4$.
- Block glulam beams were modelled in which the width over height relation was:
 - 400 mm x 400 mm,
 - 400 mm x 600 mm, 600 mm x 600 mm,
 - 400 mm x 800 mm, 600 mm x 800 mm, 800 mm x 800 mm
- Finally, some simulations were made in which the pith location was varied using a mean and standard deviation of the distance to the board and eccentricity. This was done using a normal distribution. The standard deviation was 12.5 mm.

Although the MIS in the middle of large cross sections are expected to reduce due to increasing width, the developments are not well understood yet. Until now, and increasing relation between potential stresses in the middle of cross section was seen as one board spanned the

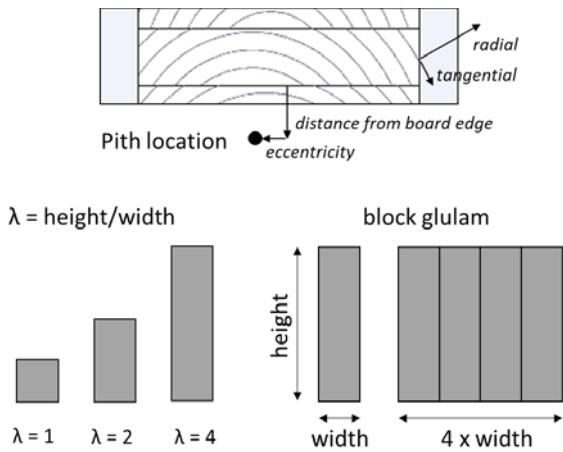


Figure 7: Illustration of a close-up of a board in a glued laminated beam with the annual ring orientation, pith eccentricity and distance from the board edge. Aspect ratio and the sideways assembly of individual beams into a block glulam beam is also illustrated.

total width of the cross section. Studies were also performed in which stresses in cross sections were mentioned to be maximum as widths were around 150 mm, and lower at 90 mm and 200 mm width [16].

4 RESULTS

4.1 EXPERIMENTS

The moisture distribution in the cross section for the three different climates in which the block glulam beam was maintained is seen in Figure 8. Each change of the ambient conditions is reflected in the change of moisture content. However, this is only observed in the outer zone of the cross section, up to 70 mm from the surface. During the strong adsorption and desorption phase the moisture content stays quite constant in the inner cross section. As the beam was placed in sheltered conditions in December, a wetting process is seen again which is followed by drying during the spring and summer months. Moisture content measurements made through the electrical resistance method are expected to have an accuracy within 2 M% [23]. This is due to material density, calibration curves, and temperature effects. If possible, a vertical offset of the time traces can be added only after finishing the test series, using the oven dry methods. This would improve the accuracy of the absolute values. Due to the size of the beam, specimens close to the electrode locations could not easily be obtained.

Figure 9 shows strains observed in tangential direction for all climate loading phases. Here too, the long adsorption period and desorption period are distinguished in the time traces. Whereas the strain is positive close to the outer surface indicating an expansion during the adsorption process, within the cross section, a compression is observed. This is opposite for the desorption process. During the placement in the outside climate, the strains in close to the outer surface and in the inner cross section are opposite again. The translation to what levels are realistic in terms of stress still needs to be made. Hygro-expansion and elasticity need to be considered in this, as

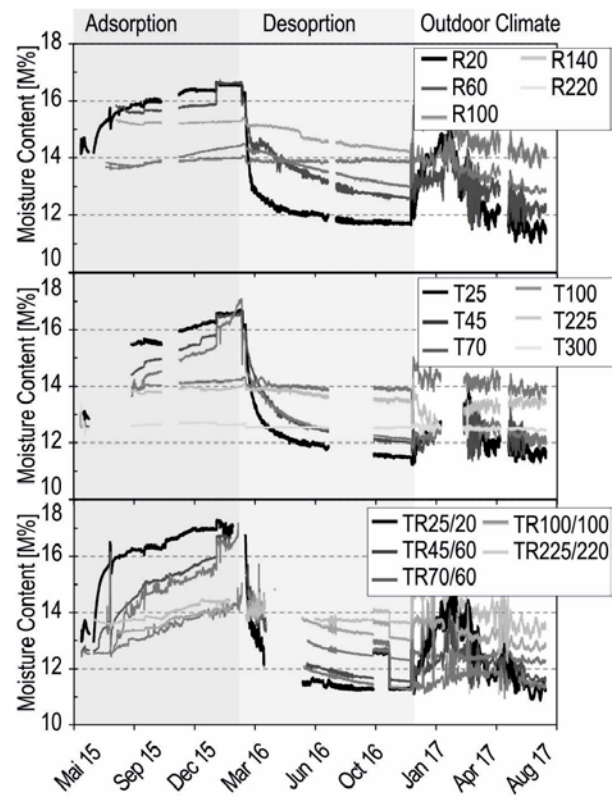


Figure 8: Measuring curves of block glued glulam member, (adjusted/cleaned curves)

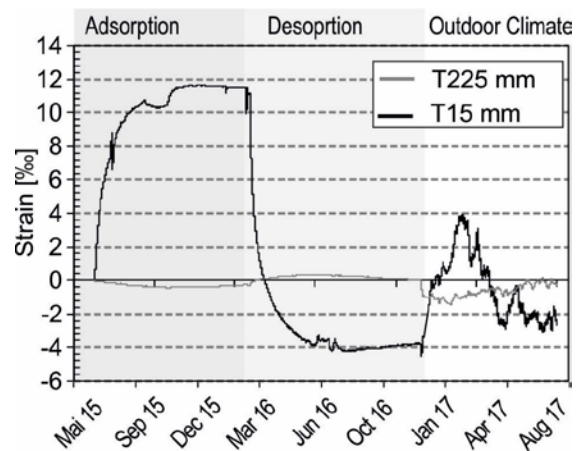


Figure 9: Strain behaviour in tangential direction, close to surface and inside of the cross section

well as the mechano-sorptive stress explained in equation (2).

The moisture content changes occurring due to the changing climatic conditions around the block glulam beam can be found in practice, perhaps not for these extended periods of time though.

4.2 STRESS DISTRIBUTIONS PERPENDICULAR TO THE GRAIN

4.2.1 Relation between cross section and developed stress distributions

As mentioned before, the MIS in the midplane of single cross sections, where the used lamellas span the total width of the beam, are expected to reduce due to in-

crease with the width of the cross section. This is because the width over which the tensile stresses internally can be distributed increases compared to the width over which the compression stresses are distributed at the outer surface. The depth into which the moisture penetrates in seasonal climatic variations is not that deep. This is complex due to the material anisotropy.

Stresses in the beam's vertical direction reduce the single beams are glued into block glulam beams, see Figure 10 (top). The figure shows the maximum stresses during the wetting and drying processes. These occur at different moments after the processes have been started.

If the lamella width spans the total width of the beam, tensile stresses in the midplane of the cross sections increase. A way to reduce this is by increasing the distance of the pith from the lamella edge. The pith distance increases as the annual ring angle with the side surface of the beam is kept constant when the lamella width increases. It was expected that if this was kept constant, tensile stress levels could remain constant as well. Gluing single beams into wider, block glulam beams, reduces tensile stresses found in the cross sections.

During desorption processes, Figure 10 (bottom), stresses at the surface are not much affected by geometry of the beam. This is seen through the almost constant tensile stress levels as the width of the cross section increases, especially when assembled into block glulam configurations. The stresses remain constant too if the annual ring angle at the surface is maintained at a constant level.

As soon as the blocks are glued together sideways, the

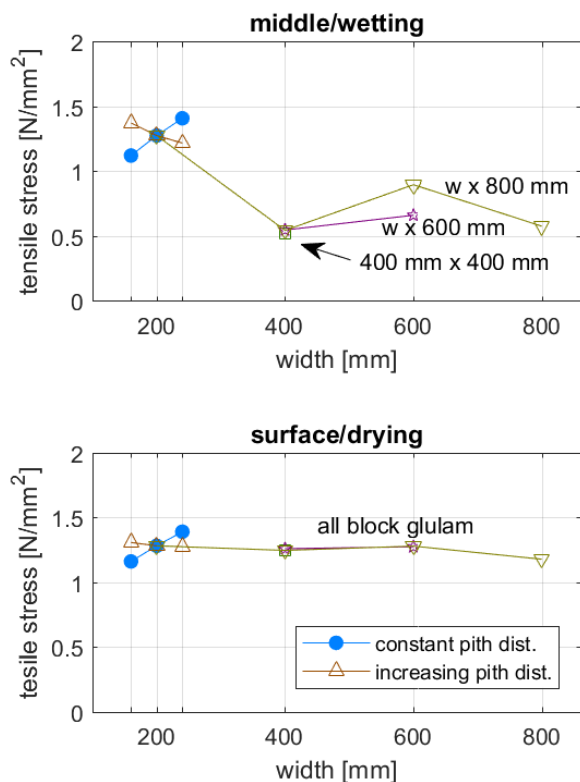


Figure 10: Comparison of maximum tensile stresses in the midplane during wetting (top) and maximum stresses in the surface during drying (bottom). Both changes were at 6 M%.

tensile stresses do not automatically show a decreasing trend as width increases. The dependency of the tensile stresses on beam geometry is further studied and explained through Figure 11. The figure shows the distributions of the stresses in vertical beam direction at the moment where the maximum tensile stresses were observed on the 800 mm high cross sections. The top figure shows that whenever the block glulam beams contain an even number of single beams, stresses are reduced in comparison to the block glulam beams with an uneven number. During drying (bottom figure), the stresses at the surface are independent of the size or geometry. This explains why cracks in beam surfaces are seen so often, on nearly any type of cross section.

The top figure of Figure 11 also shows that the stresses in the horizontal direction (σ_x), do not contribute that much to the total stress present in the center of the cross section. The calculation of the total stress was explained in Section 2.3 and Figure 6. The dashed line is only slightly higher than the continuous line that represents the stresses in vertical direction only (σ_y).

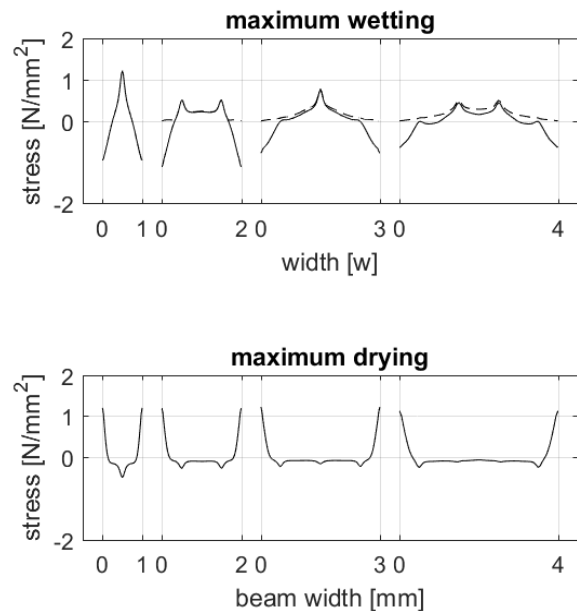


Figure 11: Illustrations of the stress distributions in vertical direction when these achieve their maximums in the midplane during wetting and maximum in the surface during drying on a 800 mm deep beam. The dashed line shows the combination of the stresses explained in Section 2.3.

The tensile stresses in the midplane during wetting take time to develop, those on the outer surface during drying don't. They occur almost immediately after the start of the drying process. This means that high tensile stresses in the midplanes develop only if the cross sections are subjected to increased humidity over long time spans.

4.2.2 Consequences of pith eccentricity

The eccentricity of the pith location with respect to the board midplane and the layout of the individual boards in a glulam beam cross section were studied too, see Figure 12. The standard deviation of the pith's eccentricity was varied from 0.0 mm in the idealised case used until now

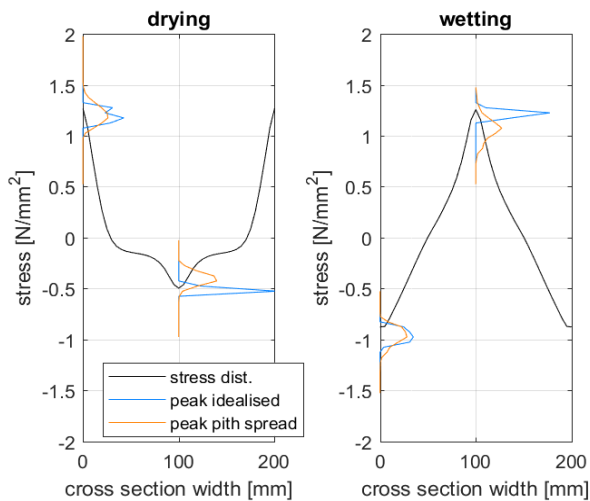


Figure 12: Calculation of internal tensile stresses in the cross section midplane and compression at the surface in wetting under different eccentricity of the pith.

to 12.5 mm further on. Studies were done still on a 200 mm wide cross section. The figure shows an average stress distribution over the cross section at the point where maximum tensile stresses are achieved. Scaled probability distributions of stresses are shown in the midplane and surface for the idealised and more realistic beam layups.

The pith's eccentricity especially affects the magnitude of the stresses on the outer surface of the beam. The maximum stresses in the middle of the cross section are hardly affected by the pith spread, both during drying processes and wetting processes. The distributions show that the mean reduces, but the spread increases. On the surface however, the maximum stresses tend to increase. The mean does not change. The spread does though, causing a net increase in the end.

5 CONCLUSIONS AND RECOMMENDATIONS

The presented research results reached in monitoring campaign provide new guidelines for the planning engineers for the assignment of service classes. The moisture content for block glued glulam cross sections used in bridges shows that the climate loads react mostly in the outer zone of the cross section. The changing ambient climatic conditions especially affect the outer surface of the glued laminated timber beams. Moisture content and strain respond quickly to a variation in the surrounding humidity. Although changes in moisture content were minimal on the inner section, strains here were measured.

The numerical study showed that tensile stress levels in the middle of the cross section are of concern. Possible cracks cannot be observed visually either. That cracks can be generated has been shown in laboratory studies and in actual structures, often found after destructive tests or complete disassembly. These are generated only after long wetting processes. Pith spread has a positive effect on the stress levels in the middle of the cross sections.

Stresses at the surface develop immediately after a change in the surrounding climate. Pith spread has a negative effect the developed stresses as the mean of these stresses does not change but the spread does. Cracks observed at the surface of cross sections are very common; either through delamination or substrate failures.

ACKNOWLEDGEMENT

The project was funded by the Swiss Fund for Forest and Forest products. The industry partners are greatly acknowledged for their participation, so is the support of the research institutes involved.

REFERENCES

- [1] SN EN 1995-1-1:2004-12; Eurocode 5: Bemessung und Konstruktion von Holzbauten Teil 1-1: Allgemeines – Allgemeine Regeln und Regeln für den Hochbau: Schweizerischer Ingenieur- und Architektenverein, Zürich, Switzerland, 2012
- [2] SIA 265:2012; Holzbau, Schweizerischer Ingenieur und Architektenverein, Zurich, Switzerland (in German)
- [3] Frese M. and Blass H.J.; Statistics of damages to timber structures in Germany, Engineering Structures 33, pp. 2969–2977, 2011
- [4] P. Dietsch and S. Winter; Structural failure in large-span timber structures: A comprehensive analysis of 230 cases, Journal of Structural Safety 71, pp. 41-46, 2018
- [5] Jönsson J.; Internal stresses in the cross-grain direction in glulam induced by climate variations, Holzforschung 58, pp. 154–159, 2004
- [6] Möhler K. and Steck G.; Untersuchungen über die Rissbildung in Brettchichtholz infolge Klimabelastungen, Holzbauauforschung, pp. 194-200, 1980
- [7] Franke B., Franke S., Müller A., Schiere M.: Long-term behaviour of moisture content in timber constructions – Relation to service classes, INTER conference proceedings 2016, Graz, Austria, 2016
- [8] Aicher S., Dill-Langer G., Ranta-Maunus A.; Duration of load effect in tension perpendicular to the grain of glulam in different climates, Holz als Roh- und Werkstoff 56, pp. 295-305, 1998
- [9] Gustafsson P.J., Hoffmeyer P., Valentin G.; DOL behaviour in end-notched beams, Holz als Roh- und Werkstoff 56, pp. 307-317, 1998
- [10] Widmann, R.; Sanierung und Verstärkung von Brettchichtholz, S-WIN-KURS 2014, Weinfelden Switzerland, 2014
- [11] Franke B., Franke S., Müller A.; Case studies: Long term monitoring of timber bridges, Journal of Civil Structural Health Monitoring (5), p. 195 - 202, 2014
- [12] Gamper A., Dietsch P., and Merk M.; Gebäudeklima - Langzeitmessung zur Bestimmung der Auswirkungen auf Feuchtegradienten in Holzbauteilen, Stuttgart, Germany, Technical report F 2816, 2012
- [13] Schiere M., Franke B., Franke S., Müller A.; Comparison between local versus regional climate using monitoring data of timber structures, WCTE 2018

- Conference proceedings, South Korea, 2018 (to be published)
- [14] Swiss timber bridges, www.swisstimberbridges.ch, 2017
- [15] Thelandersson S. and Larssen H. (editors); Timber Engineering, Wiley and Sons, ISBN: 978-0-470-84469-4, 2003
- [16] Angst-Nicollier V.; Moisture induced stresses in glulam - effect of cross section geometry and screw reinforcement, PhD thesis 2012:139, NTNU Trondheim, Norway, 2012
- [17] Häglund, M.; Moisture content penetration in wood elements under varying boundary conditions, Wood Science Technology 41, 477-490, 2007
- [18] Fortino S., Hradil P., Genoese A., Genoese A., pousette A., Fjellström PA.; A multi-Fickian hygro-thermal model for timber bridge elements under northern europe climates, WCTE 2016 conference proceedings, Vienna, Austria, 2016
- [19] Droin-Josserand A., Taverdet J.M., Vergnaud J.M.; Modelling the process of moisture adsorption in three dimensions by wood samples of various shapes, Wood Science and Technology 23, pp. 259–271, 1989
- [20] Schiere M., Dietsch P., Franke B., Franke F., Müller A.; Calculation of experimental moisture diffusion values in large glulam cross sections, Journal for Construction and Building Materials (in review), 2018
- [21] Schiere M.; Moisture induced stresses in glulam cross sections, Master Thesis, Bern University of Applied Sciences, Department of Architecture, Wood and Civil Engineering, 2016
- [22] Blass H.J. and Schmid M.; Querszugfestigkeit von Vollholz und Brettschichtholz, Holz als Roh- und Werkstoff 58, pp. 465-466, 2001
- [23] Dietsch P., Franke S., Franke B., Gamper A., Winter S.; Methods to determine wood moisture content and their applicability in monitoring concepts, Journal of Civil Structural Health Monitoring 5, 115–127, 2014